ce/papers
The online collection for conference papers in civil engineering
Ernst & Sohn A Wiley Brand

ORIGINAL ARTICLE

SDSS 2022
The International Colloquium on Stability and Ductility of Steel Structures
14-16 September, University of Aveiro, Portugal
Ernst & Sohn A Wiley Brand

A New Eurocode-compliant Design Approach for Cold-Formed Steel Sections

Dieter Ungermann[1], Tim Lemański[1], Bettina Brune[1]

Correspondence

Tim Lemański, M.Sc.
TU Dortmund
Institute of Steel Construction
August-Schmidt-Straße 6
44227 Dortmund
Germany
Email: tim.lemanski@tu-dortmund.de

Abstract

A new, Eurocode-compliant design approach based on the Direct Strength Method (DSM) combined with EN 1993-1-3 was developed for the design of thin-walled cold-formed steel sections. The new design approach transfers cross-sectional resistance according to DSM, based on numerical elastic buckling analyses on the gross cross-section, into the global stability check according to EN 1993-1-3. Experimental investigations on various perforated and unperforated cold-formed sections in compression and bending serve to verify the new design approach. In addition, a numerical model was developed, it was calibrated on the test results and used for further parametric analyses on the load-carrying capacity of cold-formed sections.

Keywords

Cold-formed steel sections, stability, EN 1993-1-3, Direct Strength Method (DSM), Experimental Analysis, Finite Element Analysis

1 Introduction

Thin-walled, cold-formed steel sections are used in a wide range of areas from industrial steel construction to rack structures and special applications in viticulture. The variety of individual cross-sectional shapes with or without corrugations, folds, grooves and stiffeners is large.

However, the great advantages of the individual design and optimization of cold-formed sections for its use in steel structures and buildings are accompanied by great difficulties in the realistic assessment of the ultimate and serviceability limit state. The design of cold-formed members and sheeting is standardized in EN 1993-1-3 [1]. This standard was basically developed for C- and Z-shaped steel sections, so that its applicability is limited for the multitude of individual cross-section shapes. Considering sections with perforations, a design according to EN 1993-1-3 is even completely impossible. Furthermore, the design according to EN 1993-1-3 is complicated due to the method of effective widths, the highly complex coupled instability modes of cold-formed sections and members, it is time-consuming, error-prone and usually provides conservative results. This prevents innovative developments and optimizations of cold-formed sections and structures.

The research report [2] presents the development of a new, simplified, Eurocode-compliant design approach for cold-formed steel sections and members in which the effective widths method according to EN 1993 is replaced by the Direct Strength Method (DSM). First, the cross-sectional resistance of cold-formed sections considering local and distortional buckling is predicted according to the DSM based on modern finite strip software for elastic buckling analysis. Afterwards the design of cold-formed structural elements in global and coupled instabilities follows the design provisions of EN 1993-1-3. The internationally established DSM has emerged from research at Cornell and Johns Hopkins University (USA), it is part of the American standardization AISI [3].

2 Buckling modes of cold-formed sections

Cold-formed steel sections in compression and bending are prone to coupled instabilities. The load-bearing behaviour is influenced by local, distortional and by various global buckling modes such as flexural, torsional-flexural and lateral-torsional buckling. Exemplarily, the relevant buckling modes of a C-shaped cold-formed section are shown in Figure 1. The signature curve presents the elastic buckling loads as a function of the half-wavelength.

Local buckling will occur if single thin-walled plane cross-sectional elements are characterized by a large ratio of plate width to plate thickness, which results in a large relative slenderness for local buckling.

Distortional buckling may occur in cold-formed cross-sections with edge or intermediate stiffeners such as lips or beads. These stiffeners serve to stiffen the plane cross-sectional elements against local buckling, but they are subject to compressive stresses and therefore in turn susceptible to buckling. Distortional buckling is mostly observed by a "closing" or "opening" of open, edge-stiffened cross-sections.

In the case of global buckling, the cross-section retains its cross-sectional

1.TU Dortmund, Institute of Steel Construction, Dortmund, Germany.

shape and buckles about the principal axes as a whole.

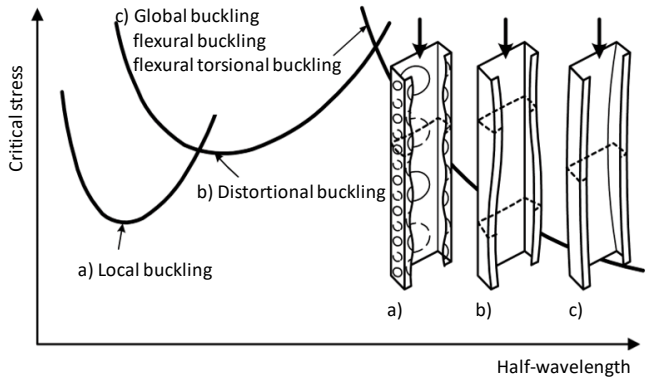

Figure 1 Buckling modes and elastic buckling stress of thin-walled cold-formed steel sections in compression

Local, distortional and global buckling modes may occur singularly, but cold-formed sections and members are mostly susceptible to coupled instabilities.

3 Standards and design approaches

3.1 EN 1993-1-3

The European design of cold-formed steel cross sections according to EN 1993-1-3 is based on effective cross-sections which cover the influence of local and distortional buckling on the cross-sectional resistance. The effective cross-sections have to be determined separately for the basic loading cases (1) axial compressive force and (2) bending moments.

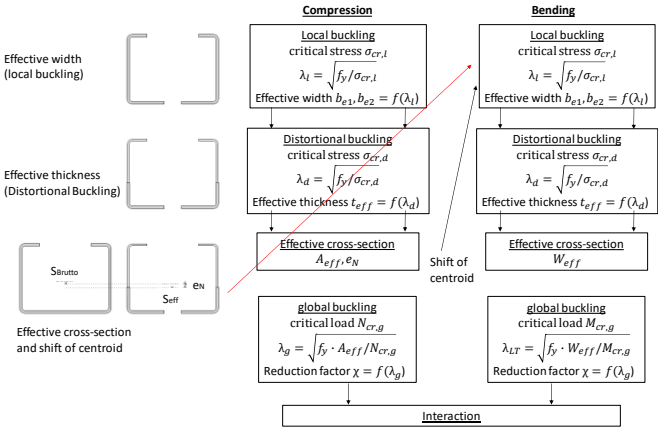

Figure 2 Flow chart of a design according to EN 1993-1-3 (Notation adjusted for better comparability)

The design starts with the determination of the effective widths of the individual cross-sectional elements due to local buckling (Fig. 2). This is followed by a thickness reduction of the compressed stiffeners to account for distortional buckling. All in all this results in an effective cross-section, which represents the cross-sectional resistance and serves as the fundamental cross-section for the global buckling design.

The centre of gravity of the effective cross-section does not always coincide with the centre of gravity of the gross cross-section. For an axial compressive force applied to centre of gravity of the gross cross-section, the effective cross-section with a shift of the centre of gravity is thus not only loaded by an axial compressive force, but by an additional bending moment ΔM. Consequently, an effective cross-section for a bending moment have to be determined in order to finally perform a verification for an interactive compressive load and bending moment.

3.2 Direct Strengh Method according to AISI

According to the DSM, the cross-sectional resistance is determined based on the gross cross-section using numerical elastic buckling analyses with the freely available finite strip software CUFSM [4]. In finit strip methods, only cross sections are modelled, it is assumed that the cross section remains unchanged along the member length. This simplification limits the application of CUFSM to unperforated sections. Alternatively, finite element software can be used to determine elastic buckling loads, which, however, is more complex, time-consuming and requires deep expert knowledge of the designer.

In agreement with EN 1993-1-3, the buckling resistance of cold-formed members has to be determined separately for the basic load cases (1) axial compressive force and (2) bending moments. Figure 3 shows the flow chart of a design according to DSM for members in compression.

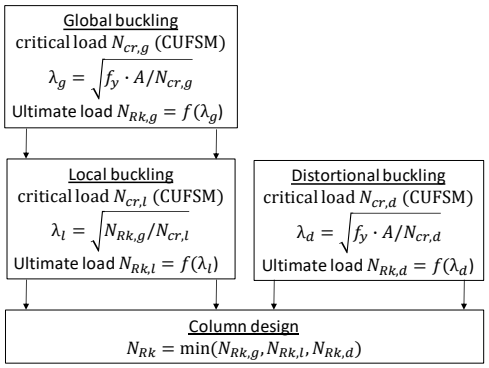

Figure 3 Flow chart of a design according to AISI DSM (Notation adjusted for better comparability)

According to the DSM, the global buckling resistance of cold-formed members due to flexural, torsional-flexural or lateral-torsional buckling is determined first. The results are introduced into the local buckling design, i.e. into the relative slenderness for local buckling. The distortional buckling resistance has to be determined separately and independent on the global-local buckling interaction. The final design value of the section´s buckling resistance according to the DSM is obtained from the minimum value of the distortional buckling resistance and the coupled global-local buckling resistance.

3.3 Comparison of the DSM and EN 1993-1-3

The European and American design provisions presented in Clause 3.1 and 3.2 differ fundamentally. The standards differ in the general order of design for different buckling modes, in the local-distortional buckling design based on effective or gross cross-sections and in the interaction of global and local instabilities. While the DSM only provides for an interaction of global and local buckling, a design according to EN 1993-1-3 covers an overall interaction of local buckling, distortional buckling and global flexural, torsional-flexural or lateral-torsional buckling. Furthermore, the effective width method according to EN 1993-1-3 covers the non-linear stress distribution of locally and distortionally buckling, thin-walled sections by the shift of the centre of gravity from the gross to the effective cross-section. The DSM only refers to the gross cross-sections, so that this essential effect is not considered.

The DSM also allows for a design of cold-formed perforated sections. Since the finite strip software CUFSM is limited to members without any perforations, see Clause 3.2, the designer has to resort to simplified approaches e.g. according to Casafont et al [5] which replace existing perforations along the member length by equivalent thicknesses. A

design of perforated members according to EN 1993-1-3 is not possible.

4 First draft of a combined DSM-EN 1993-1-3 design approach

4.1 General design procedure

The new combined DSM/EN 1993-1-3 design approach takes over the obviously advantageous design provisions of the DSM, i.e. the user-friendly, simple determination of the cross-sectional resistance dispensing with any effective cross-sections. The cross-sectional resistance predicted according to the DSM is transferred to the global buckling design according to EN 1993-1-3. In agreement with both standards, the design is initially performed separately for the load cases (1) compression and (2) bending, see Figure 4.

In a first design step, the design resistance $N_{Rk,l}$ for local buckling of a cold-formed section in uniform compression is determined according to DSM, based on the gross cross-section, see Eq.(2). The relative slenderness for local buckling λ_l depends on the elastic buckling load $N_{cr,l}$ taken from a numerical elastic buckling analysis using e.g. CUFSM, and the plastic axial force N_{pl} of the gross cross-section.

$$\lambda_l = \sqrt{\frac{N_{pl}}{N_{cr,l}}} \tag{1}$$

$$N_{Rk,l} = \begin{cases} N_{pl} & \lambda_l \leq 0{,}776 \\ \left[1 - 0{,}15 \cdot \left(\frac{N_{cr,l}}{N_{pl}}\right)^{0,4}\right] \cdot \left(\frac{N_{cr,l}}{N_{pl}}\right)^{0,4} \cdot N_{pl} & \lambda_l > 0{,}776 \end{cases} \tag{2}$$

Besides, the design resistance $N_{Rk,d}$ accounting for distortional buckling has to be predicted according to DSM in a similar way, see Eq. (3)(4).

$$\lambda_d = \sqrt{\frac{N_{pl}}{N_{cr,d}}} \tag{3}$$

$$N_{Rk,d} = \begin{cases} N_{pl} & \lambda_d \leq 0{,}561 \\ \left[1 - 0{,}25 \cdot \left(\frac{N_{cr,d}}{N_{pl}}\right)^{0,6}\right] \cdot \left(\frac{N_{cr,d}}{N_{pl}}\right)^{0,6} \cdot N_{pl} & \lambda_d > 0{,}561 \end{cases} \tag{4}$$

The lower value of the design axial forces for local and distortional buckling becomes decisive and then transferred to the global design provisions of EN 1993-1-3.

A so-called Q-factor is introduced, which relates the design axial force for local or distortional buckling in relation to the plastic axial force N_{pl}, see equation (5).

$$Q_A = \min \begin{cases} Q_{A,l} = \frac{N_{Rk,l}}{N_{pl}} \\ Q_{A,d} = \frac{N_{Rk,d}}{N_{pl}} \end{cases} \tag{5}$$

The relative global slenderness λ_g of members in coupled instabilities according to EN 1993-1-3 is based on the effective cross-sectional properties which represent the reduced cross-sectional resistance due to local and distortional buckling. Exemplarily the effective area A_{eff} is decisive for a member in compression , see Eq. (6).

$$\lambda_g = \sqrt{\frac{A_{eff} \cdot f_y}{N_{cr,g}}} \tag{6}$$

A simple reformulation results in the following equation for the relative global slenderness, depending on local and distortional buckling effects:

$$\lambda_g = \sqrt{\frac{A_{eff} \cdot f_y \cdot A}{N_{cr,g} \cdot A}} = \sqrt{\frac{A \cdot f_y}{N_{cr,g}}} \cdot \sqrt{\frac{A_{eff}}{A}} = \sqrt{\frac{N_{pl}}{N_{cr,g}}} \cdot \sqrt{Q_A} \tag{7}$$

The Q-factor in Eq.(5) corresponds to the ratio of the effective cross-section to the gross cross-section extended by the yield strength f_y.

$$Q_{A,i} = \frac{A_{eff,i}}{A} = \frac{A_{eff,i} \cdot f_y}{A \cdot f_y} = \frac{N_{Rk,i}}{N_{pl}} \tag{8}$$

In this way, it is possible to integrate the cross-sectional resistance according to the DSM into the global design provisions of EN 1993-1-3. The relative global slenderness is essential to determine the reduction factor χ according to the European buckling curves.

$$\alpha = \begin{cases} 0{,}13 \; KSL \; a_0 \\ 0{,}21 \; KSL \; a \\ 0{,}34 \; KSL \; b \quad \rightarrow \text{C – shaped sections (lipped channels)} \\ 0{,}49 \; KSL \; c \quad \rightarrow \text{U – shaped sections (plain channels)} \\ 0{,}76 \; KSL \; d \end{cases} \tag{9}$$

$$\phi = 0{,}5 \cdot \left[1 + \alpha\left(\lambda_g - 0{,}2\right) + {\lambda_g}^2\right] \tag{10}$$

$$\chi = \begin{cases} 1{,}0 & \lambda_g \leq 0{,}2 \\ \left(\phi + \sqrt{\phi^2 - {\lambda_g}^2}\right)^{-1} \leq 1{,}0 & \lambda_g > 0{,}2 \end{cases} \tag{11}$$

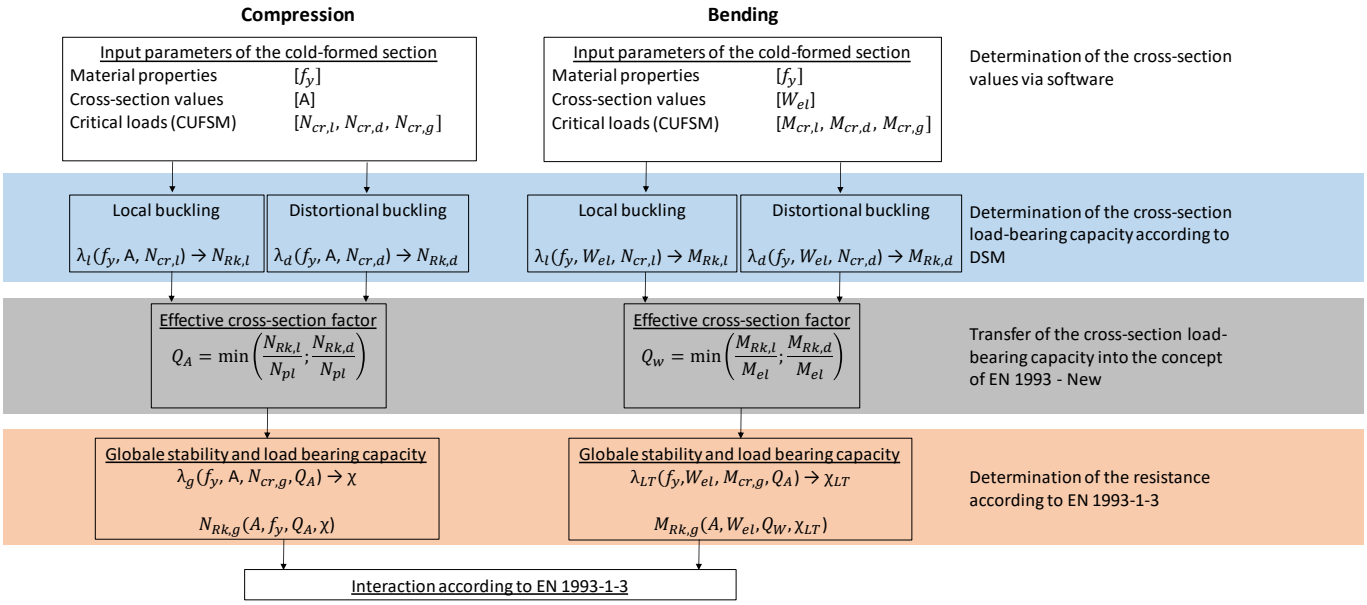

Figure 3 Flow chart of a design according to the combined design approach

The design axial force $N_{b,Rk}$ of a member in uniform compression can be determined according to Eq.(12) taking into account the relevant local-distortional buckling reduction via Q-factor and the reduction factor χ for global buckling.

$$N_{b,Rk} = \chi \cdot Q_A \cdot N_{pl} = \chi \cdot A_{eff} \cdot f_{yk} \quad (12)$$

The prediction of the design bending moment $M_{b,Rk}$ of cold-formed members in coupled instabilities ultimate limit state due to a bending stress $M_{b,Rk}$ follows the same principles using a corresponding Q-factor Q_w to consider the relevant local-distortional buckling modes and the reduction factor χ_{LT} due to lateral-torsional buckling, see Eq.(13).

$$M_{b,Rk} = X_{LT} \cdot Q_w \cdot M_{el} \quad (13)$$

For cold-formed members in interactive compression and bending the global buckling design provisions of EN 1993-1-3 can be used without restrictions.

4.2 Comparison of the first draft of the new combined design approach with the provisions of DSM and EN 1993-1-3

In contrast to EN 1993-1-3, which considers an overall interaction of local, distortional and the decisive global buckling mode, and in contrast to the DSM, which only covers an interaction of local buckling and global stability, the combined design approach considers an interaction of global buckling with the relevant local-distortional buckling mode. Local and distortional buckling is ignored according to the DSM and research of Schafer [6].

Since no effective cross-sections are determined, the potential shift of the centre of gravity from the gross to the effective cross-section is ignored and no additional bending load ΔM occur for members in axial compression.

5 Experimental analysis

5.1 Tests on cold-formed members in compression

Column tests on C- and Ω-shaped cross-sections with or without perforations were carried out to validate the new combined design approach in comparison to the DSM and EN 1993-1-3 against the test results.

Compression tests on short and medium-length columns according to EN 1993-1-3, Annex A, and EN 15512, Annex A, are performed to determine the cross-sectional resistance covering local buckling (short length) and distortional buckling (medium length). Furthermore, these tests serve to determine the optimum location of the axial load application by varying the load application on the axis of symmetry until the maximum cross-sectional resistance for local and distortional buckling is achieved. In accordance with EN 1993-1-3, Annex A, the member length of short column tests is defined as the triple plate width, while the natural half-wavelength for distortional buckling determined by finite strip analyses (CUFSM) defines the lengths of members in medium-length column tests according to EN 15512, Annex A.2.2. In addition, long column tests for members with lengths used in typical applications are used to investigate coupled instabilities and the effects on the interactive buckling resistance of cold-formed members.

As an example, the test setup for a column tests on an Ω-shaped rack upright according to EN 1993-1-3, Annex A, is shown in Figure 5 a) and b). The upright was welded to thick-walled base and cap plates. Axial spherical plain bearings between the base/cap plates and connecting plates serve to realize a simple support. The load was applied via the welded cap plates, which were bolted to a connecting plate using slotted holes to shift the location of the applied axial load, see Figure 5 c.

During the test, strains were measured at minimum three locations across the member using strain gauges. Local horizontal displacements of the cold-formed section were recorded via several inductive displacement transducers. The load was applied in a displacement-controlled manner in order to stress the specimen and to analyse the load-bearing behaviour beyond the ultimate resistance.

Figure 6 shows the remaining failure patterns of C-shaped cross-sections in compression with different lengths after testing and unloading. As expected, local buckling was the dominant buckling mode for short columns. At medium length, distortional buckling dominated. In the buckling tests with large global slenderness, flexural-torsional buckling about the major axis became decisive.

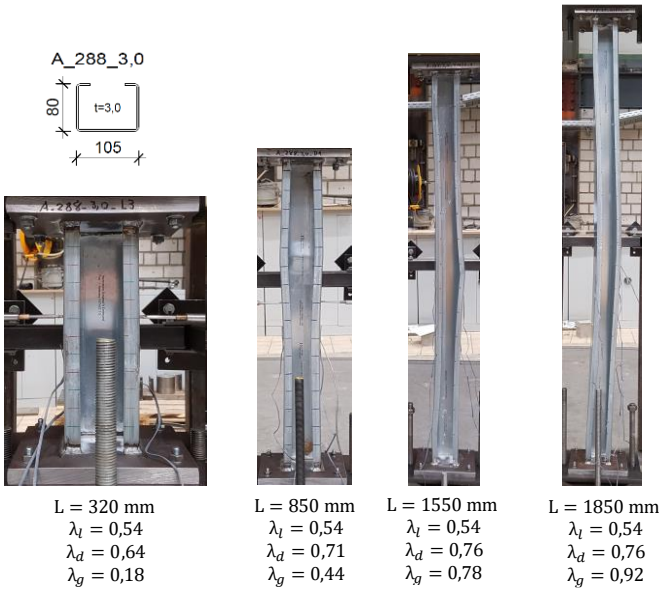

Figure 6 C-shaped cross-section in all examined lengths after unloading

The tests with medium length L=1550mm (global slenderness $\lambda_g = 0{,}78$)

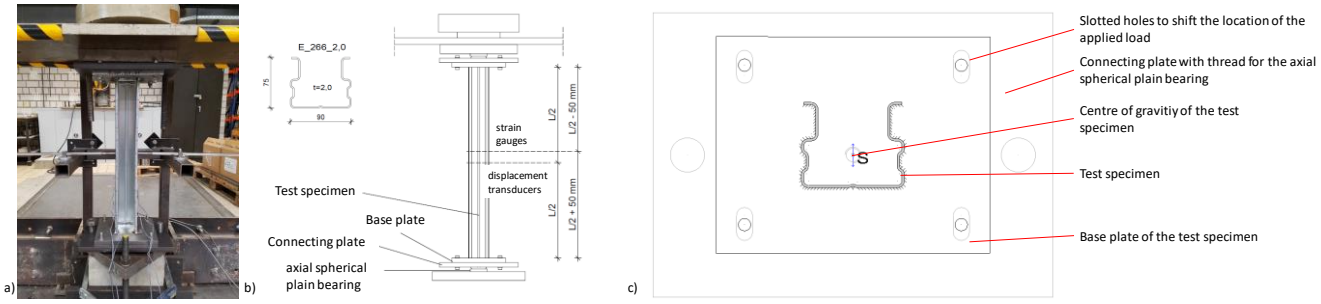

Figure 5 Test setup of the compression tests a) Ω-shaped cross-section in the test setup b) Construction sketch of the test setup c) Realization of the load application

prove an interactive flexural-torsional and distortional buckling, contrary to the specifications of the DSM.

The initial tests applying the axial force at different locations on the symmetry axis confirmed the shift of the internal compressive force resultants due to local and distortional buckling. The maximum cross-sectional capacity for a tested C-shaped section with a length of 420 mm was achieved when the axial load was applied 8mm away from the centre of gravity of the gross cross-section, see Figure 7 a). Ignoring this effect in the design of cold-formed sections could lead to falsified results.

A total of 79 compression tests were carried out as part of the research project. Detailed results and documentation can be taken from the final report [2]. Key exemplarily test results and corresponding verifications according to the new design approach of Clause 4 compared to the provisions of EN 1993-1-3 and the DSM are summarized in Figure 7 c), d), e). In order to achieve realistic design results, the FE software ANSYS (version 2020 R2) [7] was used to calculate elastic buckling loads. This allows the special boundary conditions in the tests to be recorded accurately. For better comparability of the different design results, partial safety factors were ignored and a uniform Young's modulus of 210,000 N/mm² was applied. The measured imperfections along the tested members, corresponding to global buckling modes of the specimens, were quite low, therefore the favourable European buckling curve *a* was assumed for the global buckling design.

The design of short columns in compression prove that both the DSM and the first draft of the new combined design approach may overestimate the cross-sectional resistance if local-distortional buckling gets dominant. But the design became more conservative with increasing global slenderness. In contrast, a design according to EN 1993-1-3 proved to be too conservative for all tested sections irrespective of the member length.

Furthermore, the column tests showed that global-distortional buckling might occur, this effect is ignored in the DSM design. In addition, a shift of the compressive force resultants was identified for different types of mono-symmetrical sections at small and medium length. Ignoring this effect in the prediction of the cross-sectional resistance, as specified in the DSM, may lead to non-conservative design. Consequently, the first draft of the new combined design approach, which base on the DSM provisions for local and distortional buckling design, was adapted, see Clause 7.

5.2 Tests on cold-formed members in bending

Four-point bending tests on C-, Z- and Ω-shaped, perforated and unperforated cold-formed sections are carried out according to EN 1993-1-3, Annex A, and EN 15512, A.2.5, to investigate the design buckling resistance in major-axis bending. Since all tested sections are single-symmetrical or non-symmetrical sections, a "double" test setup was realized in accordance with EN 15512, A.2.5 [8]. Two beams were each connected by a bolted web-to-web connection at the supports and the location of load application including spacers, see Figure 8. This test setup allows the application of a vertical load into the test beams without additional torsional loading, which would be unavoidable with single-tested, single-symmetrical beams.

Figure 8 Test setup of the four-point bending tests and detail of the load application

To prevent crushing or web crippling subject to support reactions and the applied transverse forces, the sections were stiffened by steel spreadings. The sections were tested in two different lengths specified as 15 times or 30 times the section´s depth according to EN 15512, A.2.5. The shorter length was used to determine the cross-sectional resistance of the section in bending due to distortional buckling, while the interaction of global and distortional buckling was to be investigated for the longer lengths. Due to the favourable stress distribution of a cross-section in pure major-axis bending and the low plate buckling slenderness, the occurrence of local buckling was not expected.

To record and analyze global lateral-torsional buckling modes the twisting of the specimen was measured by rope displacement transducers. Measurements of the relative flange displacement with the help of inductive displacement transducers serve to investigate distortional buckling modes. Figure 9 shows an example of a Z-shaped section subject to lateral-torsional buckling at long member length (a)

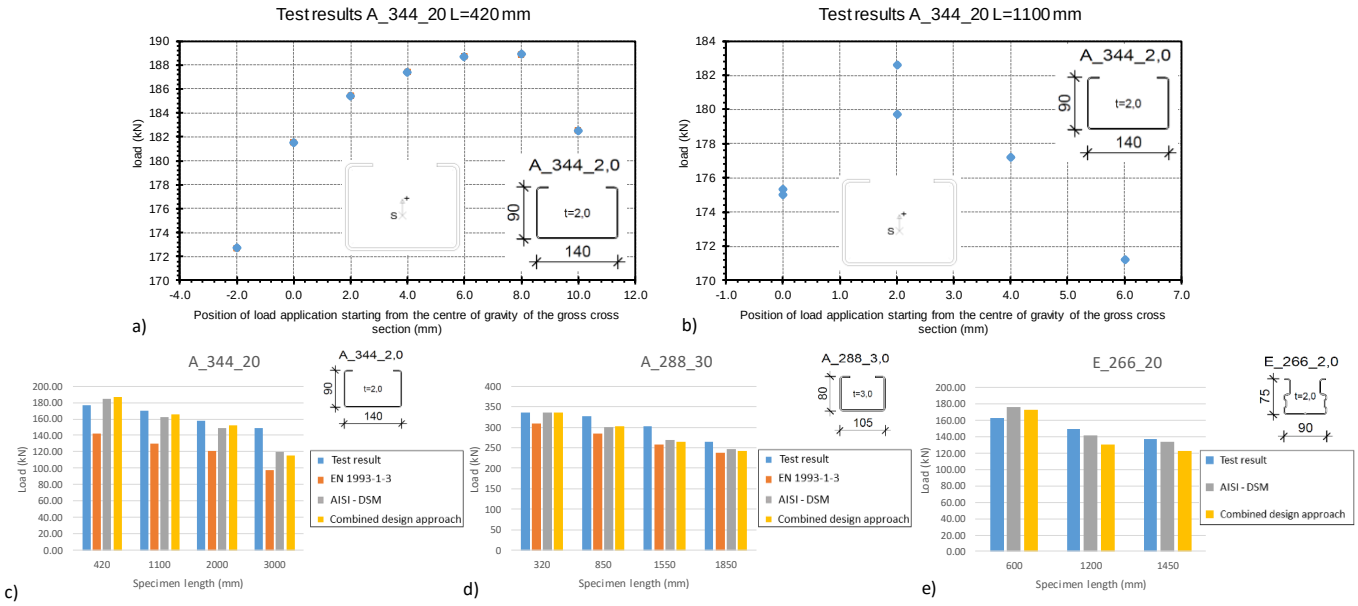

Figure 7 Results of the compression tests: Load capacity depending on load application point for A_344_20 L=420 mm [a)] and L=1100 mm [b)] Comparison of the calculation according to EN 1993-1-3, AISI DSM and he combined approach with the test results for test specimen A_344_2,0 [c)], A_288_3,0 [d)] and E_266_20 [e)]

and susceptible to distortional buckling at short member length. A total of 44 major-axis bending tests were carried out in the research project, see [2].

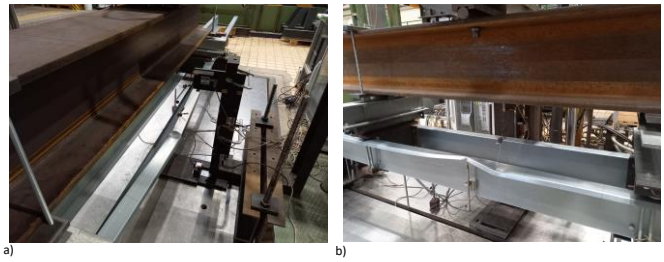

Figure 9 Test specimen (Z-shaped section) after testing and unloading a) lateral-torsional buckling at long length b) distortional buckling at short length

Figure 10 shows a comparison of the test results of C- and Ω-shaped sections in major axis bending with design predictions according to the new combined design approach, EN 1993-1-3 and the DSM, in which the relevant partial safety factors are set to "1,0", Young´s modulus is 210,000 N/mm² and the elastic buckling analysis is carried out with CUFSM. Since the measured global imperfections of the specimen are very small, European buckling curve *a* was applied for the global lateral-torsional buckling design according to EN 1993-1-3 which is also part of the new combined design approach. The comparison in Figure 10 proves that the DSM and the combined design approach might provide non-conservative results considering these cross sections.

Consequently, the new combined design approach also had to be improved and adapted for the design of cold-formed sections in major axis bending, see Clause 7.

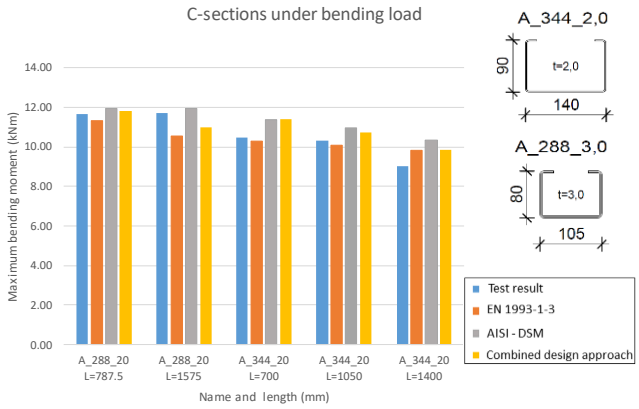

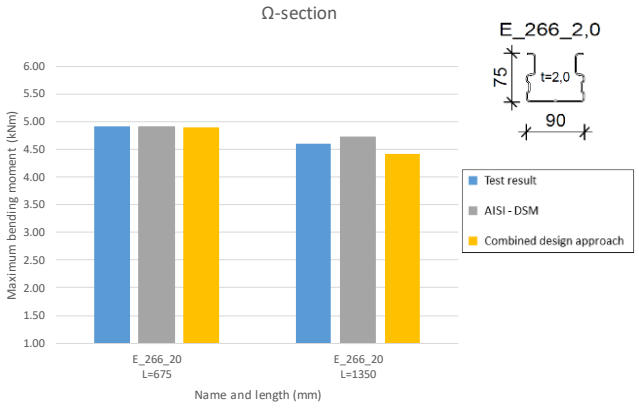

Figure 10 Comparison of the analytical calculation according to the combined design approach, EN 1993-1-3 and AISI DSM with the test results

6 Numerical analysis

Numerical models using ANSYS 2020 R2 were developed and calibrated on the test results. Parameter studies serve to further investigate and to analyze the load-carrying behaviour and the buckling resistance of cold-formed sections with varying cross-sectional dimensions, steel grades, member length and loadings in depth. For an accurate calibration of the numerical model, local, distortional and global imperfections of the specimen measured in the tests were applied.

Furthermore, the effects of strain hardening were included. Cold-formed steel sections are usually produced by roll forming or bending of pre-galvanized sheet thin-walled steel strips which cause strain hardening in the cold-formed rounded corners of the sections. Preliminary tensile tests according to EN ISO 6892-1 were carried out to record the change in material properties due to strain hardening. Two types of specimens were investigated, the first was taken from the initial steel coil, the second from the areas of the cold-formed corners of the sections. Figure 11 presents a specimen for tensile tests taken from the areas of the cold-formed corner of a C-shaped section (right). Furthermore, a comparison of the stress-strain curve of a specimen taken from the initial steel coil (blue) with a specimen taken from the rounded corner of a cold-formed C-shaped section (green) prove the increase of yield stresses due to work-hardening.

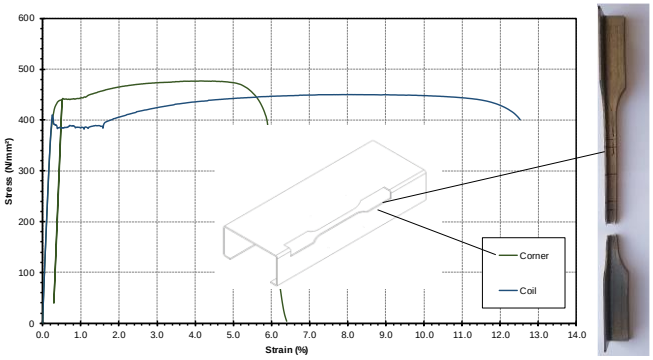

Figure 11 Comparison of stress-strain curves from an unworked specimen (Coil) to a work-hardened specimen (Corner)

The effects of work-hardening are covered in the numerical model by dividing cold-formed sections into hardened and unworked areas where bilinear characteristic material models with different material parameters resulting from the tensile tests were applied.

Figure 12 shows the material assignment on a tested Ω-shaped cross-section in compression and the corresponding numerical model. The test specimen, including base and cap plates, was modelled with shell elements. Corresponding to the column tests, the axial load was applied through the cap plates corresponding to the column tests. The cold-formed member was vertically and laterally supported in the centre of the column base. The symmetry axis of the cap plates was fixed in the z-direction and an additional displacement in the y-direction was blocked at the location of the load application. This modelling generates simple support conditions and allows the head plate to rotate about both the z- and y-axes.

The numerical model of cold-formed sections in bending does not cover the applied double member test, but concentrates on simulations of only one specimen by using symmetry conditions. Corresponding to the bending tests, the transverse load was applied via spacers at the location of the bolted connections, see Figure 12 (right). The spreaders used in the tests to avoid web crippling and flange deformations where applying

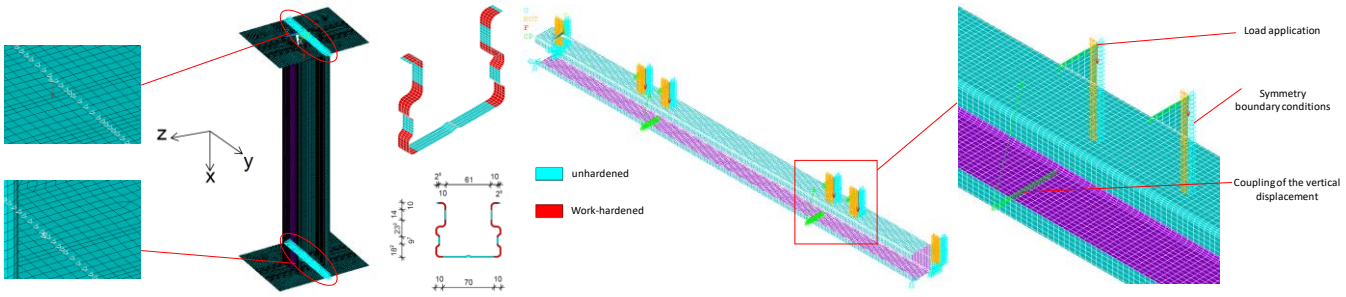

Figure 12 Numerical model of compression tests, approach of material hardening and numerical model of four-point bending tests (from left to right)

transverses load were modelled by coupled displacements of the lower and upper flanges.

The results of the finite element simulation are in very good agreement with the test results of both compression and bending tests of cold-formed sections. The ultimate load as well as the decisive buckling or failure mode were realistically reproduced. Figure 13 shows the deformations of an Ω-shaped cross-section in compression according to tests and compared to simulations.

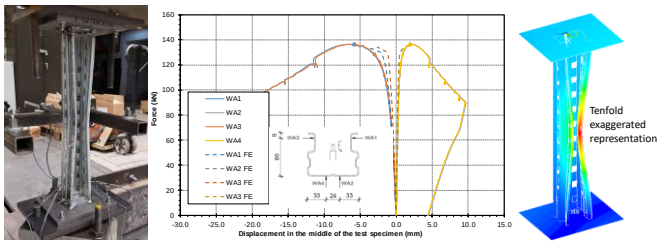

Figure 13 Results of tests and simulations for an Ω-shaped cross-section in compression

The deviation of the simulation from the test results was only about 4% caused by simplified assumptions underlying the numerical model, e.g. the simplified bilinear material model for steel. Finally, the developed numerical models can be considered as sufficiently calibrated.

Further parametric studies focussed on cold-formed sections in axial compression and the effect of the changing, finally non-linear compressive stresses due to local and distortional buckling. This effect leads to a shift of the resulting axial force after integrating the non-linear buckling stresses, see Clause 3.1. Since the analyses focussed on local and distortional buckling, only local and distortional imperfections of the individual plane elements were applied in these FE-simulations. Both, tests and FE-simulations prove that the maximum cross-sectional resistance of thin-walled members in compression mostly occurs if the axial load is applied eccentrically to the centre of gravity of the gross cross-section. It was also shown that the optimum location of the load application changes at different lengths. Figure 14 (left) presents the optimum load position of an Ω-shaped section in axial compression, related to the gross centre of gravity, at which the largest cross-sectional resistance was achieved in the simulations, depending on the member length. The largest shift of the internal axial force was recorded at a member length of 600 mm. This corresponds to the half-wavelength for elastic distortional buckling which is the relevant buckling mode in this case. As the member length and the global buckling slenderness increases, global buckling becomes dominant and local-distortional buckling decrease. The maximum buckling resistance of long members is obtained when applying the axial load approximately at the gross centre of gravity. This conclusion is in good agreement with the outcomes of the test analyses and comparing design predictions, see Figure 7. It was shown that the design predictions give non-conservative results for cold-formed members at short lengths if the obviously relevant shift of the axial forces resulting from local-distortional buckling effects was ignored. On the other hand, the design provision were confirmed when global buckling dominates and the shift of loading is negligibly small.

In the following simulations and parametric studies, the influence of different cross-sectional types in various dimensions, material and member lengths was investigated. The analyses cover C- and Ω-shaped sections in compression as well as Z-, C- and Ω-shaped sections in major axis bending. In order to be able to reproduce the load-carrying and buckling behaviour as realistically as possible with the help of the FE simulations, the findings from the initial model calibration were transferred generally to all numerical models. Young´s modulus was reduced to 200,000 N/mm² in accordance with the knowledge gained from the experimental investigations. Strain hardening in the cold-formed corner areas was taken into account, but using the simplified average yield strength according to EN 1993-1-3. Global and local imperfections were applied in accordance with the specifications of EN 1993-1-5 [9] with reference to the National Annex of EN 1993-1-1 [10]. Since EN 1993-1-5 does not provide an approach for imperfections corresponding to distortional buckling, the established approach of Rasmussen, Gilbert [11], based on Walker´s proposal for local imperfections [12], was applied. The maximum imperfection of the lips S_{0d} according to Eq.(14) results from the thickness t, the yield strength f_y and the elastic buckling stress for distortional buckling $\sigma_{cr,d}$.

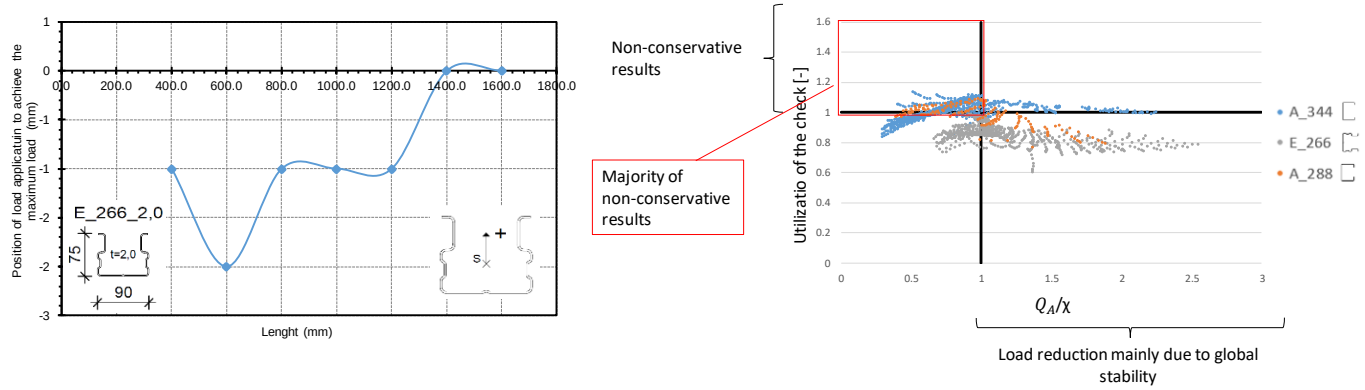

Figure 14 Results of the parameter study under compressive load

$$S_{0d} = 0{,}3 \cdot t \cdot \sqrt{\frac{f_{yb}}{\sigma_{cr,d}}} \quad (14)$$

According to the specifications of EN 1993-1-5, the relevant leading imperfection was assumed to be 100%, while other accompanying imperfections were reduced to 70%. Since the calibration of the numerical models had already proved that the imperfection approach for local buckling is very conservative, local imperfection were always defined as a companion imperfection. It became obvious that the interaction of sections with large member length and additional large local plate imperfections produced very conservative simulation results.

Figure 14 (right) shows the results of simulations and design according to the first draft of the new combined design approach for C- and Ω-shaped sections in compression and bending. The verification of the buckling resistance for members in coupled instabilities compared with the FE-simulations are recorded as a function of a newly introduced factor Q_A/χ . According to the draft of the combined design approach, Q_A was defined as a reduction factor for the cross-sectional resistance compared to the full plastic capacity of the cross-section, see Clause 4. χ is specified as the global buckling reduction factor according to the European buckling curves. The diagram proves that most of the non-conservative design results of the combined design approach occur for $Q_A/\chi \leq 1.0$. The parameter studies for cross-sections in major axis bending show similar results and lead to a similar conclusion, see [2].

7 Final improvement of the combined design approach

As a consequence of the analyses in Clause 5 and 6 the first draft of the combined design approach, derived in Clause 4, had to be adjusted to prevent non-conservative design results. The missing consideration of the shift of the nonlinear stress resultants due to local and distortional instabilities was identified to be the crucial source of error, especially for cold-formed sections at small and medium member length, whereas this effect significantly decreases with increasing member length and increasing global buckling slenderness. Therefore, the new combined design approach was extended by two new reduction factors χ_{eN} for members in axial compression and χ_{eM} for members in bending, see Eq. (14)(15). These factors will reduce the design buckling resistance, if local and distortional buckling of cold-formed cross-sections, represented by the Q-factor, become dominant compared with global buckling effects, represented by χ taken from the European buckling curves.

$$\chi_{eN} = \max[1 - \chi + Q_A; 0{,}85] \leq 1{,}0 \quad (14)$$

$$\chi_{eM} = 1 - \chi_{LT} + Q_w \leq 1{,}0 \quad (15)$$

Finally, the buckling resistance of cold-formed members in compression and bending is obtained from Eq. (16) and Eq. (17).

$$N_{b,Rk} = \chi \cdot Q_A \cdot N_{pl} \cdot \chi_{eN} \quad (16)$$

$$M_{b,Rk} = \mathrm{X}_{LT} \cdot Q_w \cdot M_{el} \cdot \chi_{eM} \quad (17)$$

8 Validation of the new combined design approach

To verify the new DSM and EN 1993-1-3 combining design approach, finally improved in Clause 7, the design predictions were carried out again and validated based on test results of Clause 3 and on the numerical simulations of Clause 6. A comparison of test results [2] with design predictions according to the new combined design approach is provided in Table 1.

Furthermore, Figure 15a-c show the comparisons of the design predictions according to the initial draft of the combined design approach (Clause 3) and the predictions according to the new improved combined design approach (Clause 7) with tests of cold-formed C- and Ω-shaped sections in compression [2]. Elastic buckling loads were determined with CUFSM in all cases. It is obvious that the buckling resistances of compressed members in coupled instabilities can be slightly reduced by the new factor χ_{eN}, non-conservative predictions for small and medium-lengths columns can now be avoided. By definition, the design of long members susceptible to dominant global buckling is not affected by this amendment.

Similar positive conclusions can be drawn from the comparison of test results with new design predictions for cold-formed members in bending, see Figure 15d-e.

Considering the C-shaped section A_344_2,0 in bending, see Figure 16d, the importance of the new reduction factor χ_{eM} becomes clear. Due to the high local slenderness and the dominant local-distortional buckling effects, the application of the new factor χ_{eM} and the reduction of the design buckling resistance within the new combined design approach to account for the nonlinear buckling stresses is essential to generate reliable design. However, this conclusion also applies to the application of the DSM, which fundamentally neglects these effects.

The comparison of simulation results with the design verifications according to the new design approach for cold-formed sections in

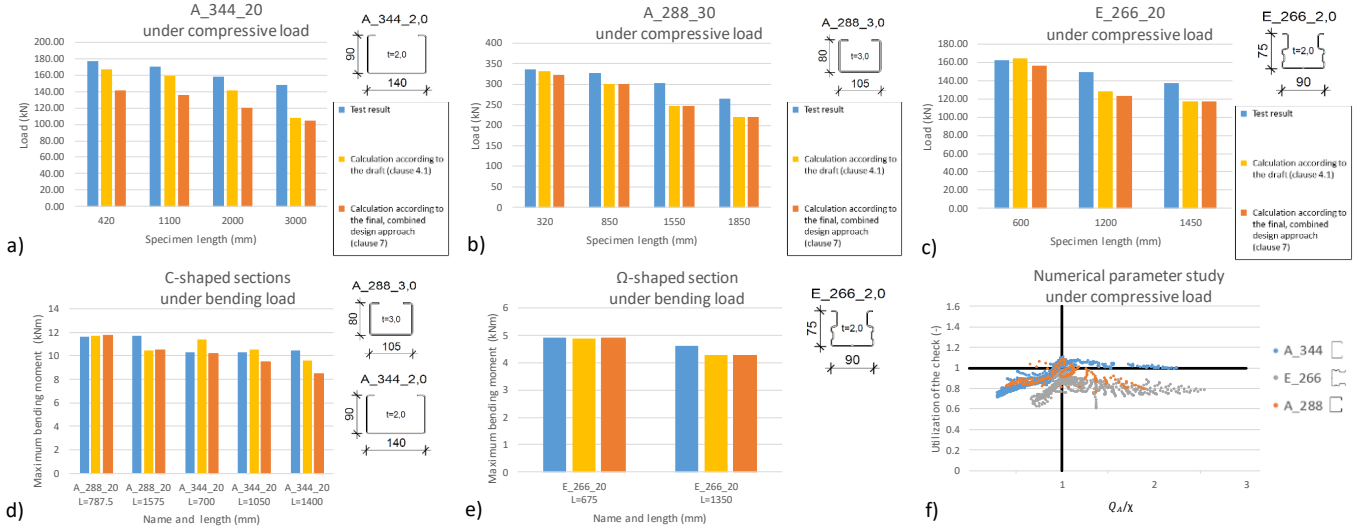

Figure 15 Comparison of the calculations according to the combined design concept and according to the draft in comparison to the test ultimate load under compressive load for different sections [a), b), c)] and for bending load [d); e)] and results of numerical parameter study in comparsion ti the combined design approach [f)}

Table 1 Overview of the results of the compression und bending test and over the calculation results according to the combined design approach

Compression								Pictograms of the cross sections
Section	Material	Length [mm]	statisitical evaluation of the normalized test results N [kN]	combined design approach				
				λ_l	λ_d	λ_g	Load capacity N [kN]	
A_288_30	S390GD+Z	320	336.22	0.54	0.64	0.18	323.27	
		850	326.50	0.54	0.71	0.44	299.87	
		1550	302.49	0.54	0.76	0.78	247.42	
		1850	263.86	0.54	0.76	0.92	220.46	
A_344_20	S390GD+Z	420	176.98	1.11	1.24	0.15	141.63	
		1100	170.30	1.11	1.24	0.39	135.49	
		2000	158.21	1.11	1.24	0.69	120.44	
		3000	148.39	1.11	1.24	1.03	105.04	
E_266_20	S350GD+Z	600	162.27	0.28	0.75	0.38	156.63	
		1200	149.03	0.28	0.91	0.7	122.93	
		1450	137.25	0.28	0.91	0.84	116.95	
E_266_20_P	S350GD+Z	600	126.84	0.35	0.81	0.41	131.12	
		1100	123.46	0.35	1.00	0.73	113.43	
		1300	114.04	0.35	1.00	0.85	103.66	
Bending								
Section	Material	Length between load application [mm]	statisitical evaluation of the normalized test results M [kNm]	combined design approach				
				λ_l	λ_d	λ_{LT}	Load capacity M [kNm]	
A_288_30	S390GD+Z	687.5	11.65	0.39	0.58	0.51	11.73	
		1475	11.69	0.39	0.49	0.24	10.48	
A_307_20	S390GD+Z	950	9.67	0.54	0.85	0.38	5.84	
		2000	7.87	0.54	0.85	0.78	5.41	
A_344_20	S390GD+Z	600	10.47	0.67	0.82	0.19	10.17	
		950	10.30	0.67	0.87	0.30	9.47	
		1300	9.01	0.67	0.95	0.39	8.44	
A_385_20	S390GD+Z	1400	13.65	0.74	0.98	0.79	9.21	
		2150	14.13	0.74	0.98	0.51	9.13	
E_266_20	S350GD+Z	575	4.92	0.20	0.59	0.22	4.88	
		1250	4.60	0.20	0.72	0.46	4.26	
E_266_20_P	S350GD+Z	575	3.77	0.25	0.61	0.23	3.10	
		1250	3.40	0.25	0.80	0.47	2.81	

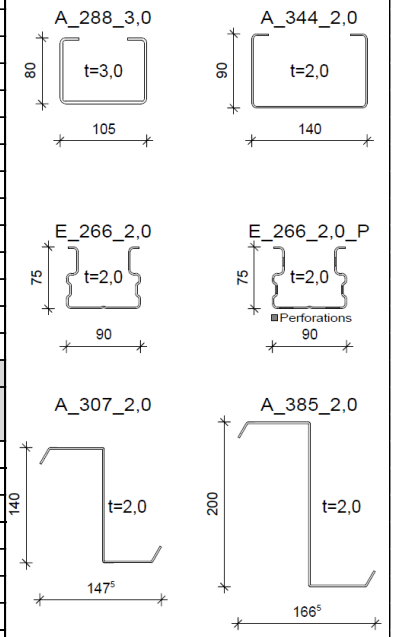

compression proves that non-conservative design can be avoided by introducing the new factor χ_{eN}, see Figure 16 f. Nevertheless, some slightly non-conservative predictions in the range of $Q_A/\chi \approx 1{,}0$ were still obtained compared with numerical simulations. However, since the simulations were generally rather conservative compared to the test results, the new combined design approach is acceptable.

9 Summary and conclusion

In this paper, a new design approach for cold-formed sections in coupled instabilities, which combines the advantages of the AISI-Direct Strength Method DSM with the design provisions of EN 1993-1-3, is presented. The cross-sectional resistance effected by local and distortional buckling modes is predicted with the help of the DSM, which is based on elastic buckling analyses using finite strip methods. The complicated determination of effective cross-sections according to Eurocode is no longer required. The global buckling design, based on the previously determined cross-sectional resistance according to the DSM, is then carried out using the design provisions of EN 1993-1-3.

Additional reduction factors χ_{eN} and χ_{eM} have been introduced into the new approach to cover the effects of the non-linear local and distortional buckling stresses in thin-walled cross-sections on the buckling resistance, which is typically ignored according to a DSM design.

Experimental investigations [2] and numerical analyses using ANSYS 2020 R2 were compared with the predictions of the new, combined design approach. Finally, it was confirmed by research that the newly developed Eurocode-compliant design approach, which favourably combines the advantages of the DSM with those of EN 1993-1-3, provides reliable buckling resistances of cold-formed sections in coupled instabilities.

With a view to the daily design in engineering practice, the new combined design approach is evaluated as simple, user-friendly, less error-prone, time-saving and efficient. It allows optimizations and even new developments of cold-formed cross-sections and shapes in a reasonable time. All in all, it is a very good alternative to the current design provisions of EN 1993-1-3 and thus recommended for an inclusion into EN 1993-1-3.

10 Acknowledgement

The research project IGF no. 19964 N / FOSTA P1328 "Future viability of cold-formed steel sections in building structures" of the Research Association for Steel Application (FOSTA), Sohnstraße 65 in 40237 Düsseldorf, Germany, was funded by the German Federation of Industrial Research Associations (AiF) as part of the program for the promotion of Industrial Collective Research (IGF) by the Federal Ministry of Economic Affairs and Climate Action on the basis of a decision by the German Bundestag.

References

[1] EN 1993-1-3 (2010) *Eurocode 3: Bemessungs und Konstruktion von Stahlbauten – Teil 1-3: Allgemeine Regeln – Ergänzende Regeln für kaltgeformte Bauteile und Bleche.* DIN Deutsches Institut für Normung e.V., Berlin

[2] Ungermann, D.; Lemanski, T.; Brune, B. (2022) *Zukunftsfähigkeit von kaltgeformten Stahlprofilen im Bauwesen.* IGF-Nr. 19964 N, FOSTA P1328

[3] AISI (2016) *Specification for the Design of Cold-Formed Steel Structural Members – Appendix 1 – Design of Cold-Formed Members Using the Direct Strength Method.*

[4] CUFSM (Software) *Cross-Section Elastic Buckling Analysis, Version 5.04, Thin-walled Structure Group, Civil and Systems Engineering, John Hopkins University: https://www.ce.jhu.edu/cufsm/downloads/*

[5] Casafont, M.; Pastor, M. M.; Roure, F.; Bonada, J.; Peköz, T. (2013) *Design of Steel Storafe Rack Columns via the Direct Strength Mehtod.* Journal of Structural Engineering, p. 669-679

[6] Schafer, B.W. (2008) *Review: The Direct Strength Method of cold-formed steel member design.* Journal of Constructional Steel Research, vol. 64, No. 7, p. 766-778

[7] ANSYS (Software) *Version 2020 R2. ANSYS Inc.*

[8] DIN EN 15512 (2021) *Ortsfeste Regalsysteme aus Stahl – Verstellbare Palettenregale – Grundlagen der statischen Bemessung.* DIN Deutsches Institut für Normung e.V., Berlin

[9] EN 1993-1-5 (2010) *Eurocode 3: Bemessungs und Konstruktion von Stahlbauten – Teil 1-5: Plattenförmige Bauteile.* DIN Deutsches Institut für Normung e.V., Berlin

[10] EN 1993-1-1/NA (2010) *Nationaler Anhang – National festgelegte Parameter. Eurocode 3: Bemessung und Konstruktion von Stahlbauten – Teil 1-1: Allgemeine Regeln und Regeln für den Hochbau.* DIN Deutsches Institut für Normung e.V., Berlin

[11] Rasmussen, K. J. R.; Gilbert, B. P. (2013) *Analysis-Based Design Provisions for Steel Storage Racks.* Journal of Structural Engineering, 139, No. 5

[12] Walker, A. (1975) *Design and analysis of cold-formed sections.* London: International Textbook Company